



Empirical seismic fragility function for fire doors based on inspection data from the 1995 Kobe earthquake and its use in post-earthquake fire risk assessments

Tomoaki Nishino^{a,*}, Aya Hada^a, Hiroshi Kawase^b, Shinichi Matsushima^a

^a Disaster Prevention Research Institute, Kyoto University, Gokasho, Uji, Kyoto 611-0011, Japan

^b General Building Research Corporation of Japan, 5-8-1 Fujishirodai, Suita, Osaka 565-0873, Japan

ARTICLE INFO

Keywords:

Fire following earthquake
Fire door
Fragility function
Seismic response analysis
Fire risk

ABSTRACT

The seismic damage to fire protection systems heavily affects post-earthquake fire safety, an important requirement for seismic-resilient buildings. Quantitative fire risk assessments are useful in understanding and improving safety. Such assessments require modeling the seismic fragility of fire protection systems. As a starting point for rigorous risk assessments, this study focuses on fire doors, which contribute to compartmentalization during fires as an underlying principle in the fire safety design of buildings; accordingly, fire door inspection records for five mid-rise buildings that suffered slight to severe structural damage from the 1995 Kobe earthquake in Japan are analyzed. The objectives of this study are to (1) develop an empirical fire door seismic fragility function based on the inspection records and (2) discuss the post-earthquake fire risk of buildings via a hypothetical case study using the developed function in terms of the loss of life caused by fires. Structural response analyses based on synthetic ground motion waveforms and Japanese building models allow the fire door damage states recorded floor by floor to be correlated with the simulated peak inter-story drift angles. The developed fragility function indicates that 50 % of fire doors fail to open or close at a peak inter-story drift angle of approximately 0.01 rad. For buildings with two exit stairways compartmentalized by smoke detector-activated fire doors, the case study reveals (1) that the post-earthquake fire risk can increase by up to 2000 times relative to normal periods because of the increased probability of ignition and the reduced reliability of the fire door system and (2) that, even if the structural response can be reduced by an improved seismic performance to less than a peak inter-story drift angle of 0.01 rad, the post-earthquake fire risk can still be high, up to 800 times higher than the normal level. These results indicate that, in addition to seismic designs aimed at reducing the structural response, the implementation of post-earthquake ignition prevention measures and the enhancement of occupant initial fire-fighting capabilities are essential for post-earthquake fire risk reduction.

1. Introduction

In addition to structural safety and business continuity, post-earthquake fire safety is an important consideration in enhancing the seismic resilience of buildings. In recent decades, earthquakes have caused damage to nonstructural building components, including

* Corresponding author.

E-mail address: nishino.tomoaki.3c@kyoto-u.ac.jp (T. Nishino).

<https://doi.org/10.1016/j.job.2025.112362>

Received 17 June 2024; Received in revised form 6 February 2025; Accepted 12 March 2025

Available online 13 March 2025

2352-7102/© 2025 The Authors. Published by Elsevier Ltd. This is an open access article under the CC BY license (<http://creativecommons.org/licenses/by/4.0/>).

architectural, mechanical, electrical, and plumbing components, as well as structural components [1–6]. Nonstructural building components constitute a variety of systems in buildings, including those related to fire protection or life safety, as well as energy and the indoor environment. The 1994 Northridge and 1995 Kobe earthquakes are known to have caused significant damage to fire protection systems [7,8]. For example, the 1995 Kobe earthquake resulted in damage to 40.8 % of sprinkler systems and 30.7 % of fire doors [8]. Meanwhile, earthquakes have triggered multiple simultaneous fires in urban areas [9–12], suggesting that the fire ignition rate after earthquakes temporarily increases with respect to the normal level. In fact, numerous studies [13–18] have empirically modeled the post-earthquake ignition probability per floor area or person as a function of ground motion intensity measures, demonstrating much larger ignition probabilities than normal levels. Seismic damage to electrical components, including equipment and wiring, can cause various undesirable electrical events, including electrical leaks, short circuits, and overheating after power is restored, potentially leading to fires.

Large outdoor fire occurrences in earthquake-prone countries with wooden buildings, such as the fires following the 1906 San Francisco [9], 1923 Kanto [10], and 1995 Kobe [12] earthquakes, serve to motivate urban-scale fire modeling and risk analyses [19–24], which have typically focused on densely built residential areas. However, fires following earthquakes also affect mid-rise and high-rise non-residential buildings. When these buildings are subjected to earthquake shaking, they experience an increased risk of indoor fires as a result of seismic damage to fire protection systems and increased ignition potential. In particular, in the case of Japan, most ignitions following recent earthquakes have arisen from electricity-related sources [17], such as electrical appliances, equipment, and wiring, suggesting that fires following earthquakes can occur in any type of building and are not limited to densely distributed low-rise residential buildings. In fact, the over 200 fires following the 1995 Kobe earthquake included 27 fires in mid-rise and high-rise buildings; of these, 8 fires occurred in non-residential buildings with 4–11 stories [25].

Quantitative fire risk assessments, often performed for typical building fires, can also be useful in understanding and improving the post-earthquake fire safety performance of buildings. The underlying concept of fire risk is typically a product of the probability of fire occurrence and the expected consequence of a fire occurrence (e.g., casualties) [26–28]. Because fire protection systems are not perfectly reliable even in normal times [29–31], the fire risk, as the expected value of consequences per a given time period, is calculated by considering various fire scenarios depending on the success or failure of fire protection systems. For fire protection systems, the reliability of fire doors, which are implemented in fire compartment walls to limit the spread of smoke and fire, is a critical element in fire risk assessments. In particular, seismic damage to stairway fire exit doors can impede the means of egress of upper floor occupants upon the occurrence of a fire, potentially resulting in significant loss of life. To perform post-earthquake fire risk assessments, modeling the seismic fragility of fire doors is one of the foremost issues to be addressed.

Seismic damage to doors is typically considered to be a result of the building inter-story drift. The inter-story drift angle (or ratio), which is defined as the ratio of the horizontal relative displacement between two adjacent floors to the story height, has been correlated with various levels of damage to doors via experimental observations [32–37]. These studies, including tests on both fire and non-fire doors, are summarized below.

- Chang et al. [32] conducted static loading tests on emergency exit doors made of metal. These tests showed that the doors functioned smoothly when the inter-story drift angle was below 0.005 rad. However, the door lock became stuck at an inter-story drift of 0.007 rad. Furthermore, when the inter-story drift angle exceeded 0.011 rad, the door frame became severely distorted.
- Lee et al. [33] conducted quasi-static cyclic loading tests on drywall partitions with metal studs. One of the specimens included a partition with a door. The test of this specimen showed that the door became jammed at an inter-story drift of 0.01 rad. At this drift, the door frame experienced a shear distortion of 0.006 rad, causing the door panel to rotate and close the gap between the panel and the frame, resulting in the door jamming. However, when the load was removed, the door panel and frame returned to their original shapes and the door began functioning properly again. At an inter-story drift of 0.02 rad, the door lock broke and the door jammed because of the rotation of the door panel. The door lock remained broken even after the load was removed, leaving the door permanently jammed. At this drift, the door frame experienced a shear distortion of 0.01 rad.
- Forcael et al. [34] tested the configuration of a residential door corresponding to the entrances of apartments formed by slender walls or columns, which made up the structural frame of the door. The test showed that, at an inter-story drift of 0.006 rad, the door became obstructed as a result of excessive spacing, out-of-plane deformations, distortions at the door lock level, and flattening of the door frame.
- Wang et al. [35] reported the key results of shaking table and subsequent fire tests conducted on a full-scale six-story cold-formed steel wall braced building. The building included nonstructural components such as interior partition walls, fire-rated and non-fire-rated doors, and household appliances. Seven earthquake motions of increasing intensity were applied to the building. The shaking table tests showed that the fire-rated doors suffered no or minor physical damage on floors where the maximum inter-story drift angle was below 0.008 rad. However, some of the doors suffered damage, including door jamming, door frame distortion, door latch failure, or more severe states, on floors where the maximum inter-story drift angle exceeded 0.008 rad.
- Meacham [36] summarized shaking table and subsequent fire tests conducted on a full-scale five-story reinforced concrete building equipped with various nonstructural components. The building was subjected to a maximum inter-story drift angle of 0.06 rad. The fire test showed that, although the sprinkler system and most firestop systems performed well, the damage to compartmentation and egress systems resulting from the ground motions allowed smoke and fire to spread and would have prevented building occupants from escaping.
- Calayir et al. [37] conducted quasi-static cyclic loading tests on fire door sets. Their tests showed that, as the inter-story drift increased, the door hinges became excessively damaged, eventually causing the door panel to jam against the door frame. At an inter-story drift of approximately 0.005 rad, the door panel and frame began to move as a unit, preventing the door panel from

opening. At an inter-story drift of approximately 0.01 rad, the door frame distortion caused large gaps between the door panel and frame at the top corner of the door set and the door panel became jammed against the door frame. Tearing of the door frame at the door lock occurred when the inter-story drift angle exceeded 0.019 rad.

Based on the above tests, the critical values of the inter-story drift angle vary between approximately 0.005 rad and 0.02 rad, depending on the test and the damage state of interest. Such uncertainty is typically considered in risk assessments via the use of fragility functions (or curves) [38,39]. Fragility functions have been extensively developed for both structural and nonstructural components [40–44]. Nonstructural component fragility functions typically model the probability of exceeding a specific damage state as a function of a structural response quantity, often called the engineering demand parameter. In particular, Miranda [45] developed fragility functions based on data from loading tests on interior doors. These functions can be used to incorporate the seismic fragility of doors into post-earthquake fire risk assessments, in addition to their reliability in normal times considered in typical fire risk assessments. However, Miranda’s fragility functions are based on very limited test data and are not specific to fire doors. Therefore, it is unclear whether these fragility functions can explain actual damage to fire doors caused by earthquakes.

The present study focuses on on-site fire door inspection records for the 1995 Kobe earthquake [46,47] and adopts an empirical approach that correlates the fire door damage caused by the earthquake with the simulated structural response quantity of the buildings, specifically the simulated peak inter-story drift angle (PIDA). The 1995 Kobe earthquake, one of the most devastating earthquakes to have occurred in Japan, caused a “damage belt” in Kobe [48], a 20-km stretch with a width of 1 km that experienced a house collapse ratio of 30 % or more. An inspection [46,47] was conducted on 15 mid-rise or high-rise buildings in or near the damage belt by the Research Committee on Fire Safety of the Architectural Institute of Japan (AIJ). The inspector selected one enclosed exit stairway from each building and recorded the damage to the fire exit doors on each floor for the selected stairway [46,47]. Despite the value of these records, they have not yet been analyzed in detail.

The objectives of this study are to (1) develop a fire door seismic fragility function based on the AIJ’s post-earthquake on-site inspection records [46,47] and (2) discuss the ratio of the post-earthquake fire risk of buildings to the normal fire risk, i.e., the relative fire risk (RFR), using the developed fragility function. The fire doors in this study are hinged doors (i.e., swinging doors), including both doors that are kept open in normal times (i.e., smoke detector-activated doors or doors with thermal fuses) and doors that are kept closed in normal times (i.e., manual doors). The fragility function developed here is applicable to this type of fire door and focuses on its post-earthquake functionality. Specifically, several fire door damage levels are defined according to different states representing the failure of the door to open or close and the probability of exceeding each damage level, i.e., the seismic “functional” fragility, is quantified as a function of the PIDA.

To achieve the first objective, this study builds on two existing sets of tools in the field of earthquake engineering. One is the synthetic ground motion waveforms calculated by Matsushima and Kawase [49] from a complex seismic source model and a three-dimensional basin structure model. The other is the multi-lumped-mass shear building models developed by Nagato and Kawase [50] that characterize the actual yield shear strength distribution for Japanese multi-story reinforced concrete (RC) buildings

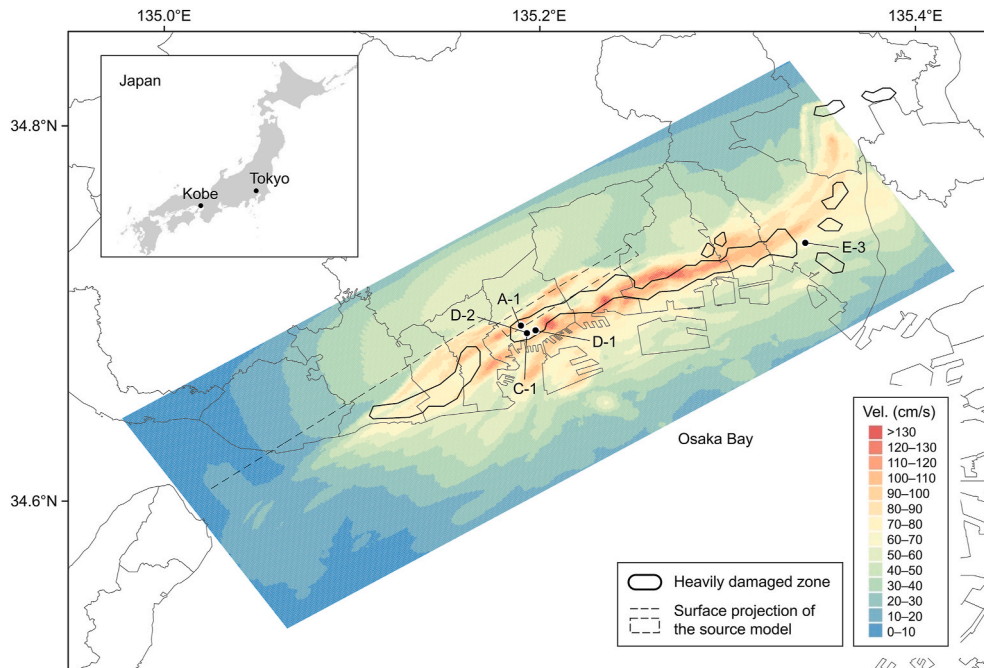


Fig. 1. Distribution of the synthesized peak ground velocities in the fault normal direction for the 1995 Kobe earthquake [49] and locations of the five analyzed buildings.

depending on the construction year and the number of stories. Using these tools, nonlinear structural response analyses are performed to estimate the PIDA for each floor and the cumulative distribution function of a log-normal distribution is applied to the relationship between the presence or absence of damage to fire doors and the estimated PIDA. To achieve the second objective, this study focuses on the loss of life caused by fires and incorporates the fire door seismic fragility function into fire risk assessments via a hypothetical case study. To simplify the discussion, an analytical equation for quantifying the RFR is derived as a function of the ground motion intensity measure and the engineering demand parameter. This newly proposed equation computes the RFR considering the probability of a stairway fire door failing to close, as well as the probability of ignition. The fire door seismic fragility function is used to quantify this door closing failure probability after an earthquake. In the case study, the effect of the PIDAs on the RFR is investigated for a hypothetical building given the context of two ground motion levels defined by the Japanese building code.

The remainder of this paper is organized as follows. Section 2 outlines the data used in the study. Section 3 describes the methodology for developing the fire door seismic fragility function, with an overview of the implemented models. Section 4 presents and discusses the developed fragility function. Section 5 illustrates the RFR assessment using the developed fragility function and discusses the post-earthquake fire risk of buildings. Finally, Section 6 presents the study conclusions and potential future work.

2. Data

2.1. Fire door inspection records for the 1995 Kobe earthquake

The fire door inspection records [46,47] contain information concerning damage to fire doors opening into enclosed exit stairways as a result of the Kobe earthquake, which struck Kobe, Japan, and its surrounding area at 5:46 a.m. (local time) on January 17, 1995, with a Japan Meteorological Agency magnitude of 7.3. As shown in Fig. 1, the 1995 Kobe earthquake caused a belt-like concentrated zone of heavily damaged or collapsed buildings, known as the damage belt. This belt stretched 20 km across the city of Kobe with a width of 1 km, was oriented west-southwest–east-northeast, and was located 1 km from the basin edge. The damage belt was found to be caused by velocity pulses that were amplified by the basin structure, that is, the amplification effect caused by the constructive interference of the direct S-wave with the basin-induced diffracted/surface waves, known as the “basin-edge effect” [48].

The fire door inspection was conducted by the AIJ Research Committee on Fire Safety from March 4 to 5 in 1995, covering a total of 15 mid-rise or high-rise buildings in or near heavily damaged areas, mostly in Chuo Ward, Kobe. The inspector selected one enclosed exit stairway in each building and, floor by floor, recorded the type (e.g., smoke detector–activated, manual, or with a thermal fuse) of fire exit door opening into the selected stairway and its damage state using a pre-developed survey form. Although no other information was reported concerning the type of fire door, such as hinged or sliding, all of the fire doors were likely hinged because they opened into enclosed exit stairways. However, they included both doors that were kept open in normal times (i.e., smoke detector–activated doors or doors with thermal fuses) and doors that were kept closed in normal times (i.e., manual doors).

As listed in Table 1, the fire door damage states were predefined focusing on the functionality of the doors and were specified on the survey form to allow the inspector to evaluate the damage objectively. The specified damage states were as follows: (1) no damage; (2) no abnormality in opening and closing, even with observed deformation and damage; (3) failure to open and close normally because of a door frame hit, floor deformation, or insufficient torque; (4) failure to close; (5) failure to open; and (6) falling off as a result of damage to the door mounting. The differences between states (3) and (4) or states (3) and (5) are not clear; however, states (4) and (5) were likely meant to report that the condition was more severe than state (3), even though the door did not fall off. In this study, the damage states were reclassified into five levels from D0 to D4, as shown in Table 1, by treating states “(4) failure to close” and “(5) failure to open” as the same level of damage because these states reflect similar damage levels. This reclassification is not expected to cause significant problems because the fragility function for state (3) is already sufficient for post-earthquake fire risk assessments given that fire doors begin to lose their functionality in state (3). Note that damage to structural components was also reported for each building, making it possible to evaluate the structural damage level of the buildings, e.g., severe, moderate, or slight. However, structural drawings are not available, limiting structural response analyses to the multi-lumped-mass shear modeling approach described below.

Of the 15 buildings surveyed, this study focuses on 5 buildings for which the Japanese building models developed by Nagato and Kawase [50] are applicable. As described below, these building models are a set of multi-lumped-mass shear models with probabilistic actual yield shear strengths; that is, the Nagato–Kawase models [50] can incorporate the uncertainty in the actual yield shear strength into the nonlinear structural response analysis. Their scope of application is limited to RC or steel framed reinforced concrete (SRC) buildings with 2–13 stories. Accordingly, this study excluded buildings with 14 or more stories and those with other types of structures,

Table 1

Fire door damage states specified in the survey form of the Architectural Institute of Japan [46,47] and damage levels reclassified in this study.

No.	Damage state	Damage level
(1)	No damage	D0
(2)	No abnormality in opening and closing, even with observed deformation and damage	D1
(3)	Failure to open and close normally because of a door frame hit, floor deformation, or insufficient torque	D2
(4)	Failure to close	D3
(5)	Failure to open	
(6)	Falling off as a result of damage to the door mounting	D4

even with 13 or fewer stories (specifically, no steel buildings; instead, mostly buildings with hybrid structures, such as upper steel and lower RC). The study also excluded buildings that experienced an intermediate story collapse because such buildings, which may have had a low yield shear strength on only a specific floor, are beyond the scope of the model.

Fig. 2 shows the observed fire door damage levels for each floor of the five analyzed buildings, along with information concerning the building construction type and year, the observed structural damage level, and the fire door type. For floors marked “D2, D3”, the fire door damage states corresponding to both levels were recorded on the survey form, indicating the possibility that the inspector determined that the damage states included both levels. The analyzed buildings were RC or SRC buildings with 8–11 stories and included buildings constructed both before and after the revision of the Japanese building code in 1981; that is, the two buildings constructed after 1981 ensured seismic performance in line with the Japanese building code, while the remaining three buildings did not. The structural damage levels of the buildings, which were inferred from the reported damage to the structural components, range from slight to severe. The fire door damage exceeded the D2 level, i.e., loss of function, on all floors in building E-3; the fire door damage occurred only on the upper or lower floors in buildings A-1, C-1, and D-1; and there was no fire door damage at all in building D-2. It is natural to assume that these different fire door damage tendencies among the buildings may have resulted from very different structural responses to the earthquake depending on the building.

2.2. Synthetic ground motion waveforms for the 1995 Kobe earthquake

Because the five analyzed buildings were distant from seismic stations and did not have their own seismic records, the synthetic ground motion waveforms calculated by Matsushima and Kawase [49] were used in this study. Matsushima and Kawase [49] numerically simulated the strong motions during the 1995 Kobe earthquake using a three-dimensional finite difference method. The simulation implemented a multiple asperity source model and a three-dimensional basin structure model. The synthesized velocity waveforms in the fault normal direction were found to agree well with those observed at most seismic stations in Kobe. As shown in Fig. 1, the simulation formed belt-like regions with high peak ground velocities, reasonably corresponding to the heavily damaged areas. Note that the synthetic waveforms were obtained on an outcrop of the Osaka Group Formation, a soft Pleistocene layer with an S-wave velocity of 400 m/s [49]. These waveforms are directly used as input motions to the analyzed buildings; that is, the amplification resulting from soft surface layers is not considered. This is because the effect of the soil amplification is expected to be set off considerably by the non-linear behavior of the soil and soil–structure interactions [49].

The Matsushima–Kawase waveforms were stored for locations at 80-m intervals. Therefore, the waveforms at the locations closest to the analyzed buildings were used. Fig. 3 shows the synthetic velocity waveforms used as inputs for each building. Note that buildings C-1 and D-2 were located near each other; therefore, the same waveforms were used. These synthetic waveforms, dominated by the fault normal component, have a common large velocity amplitude pulse with a predominant period near 1 s, similar to those observed

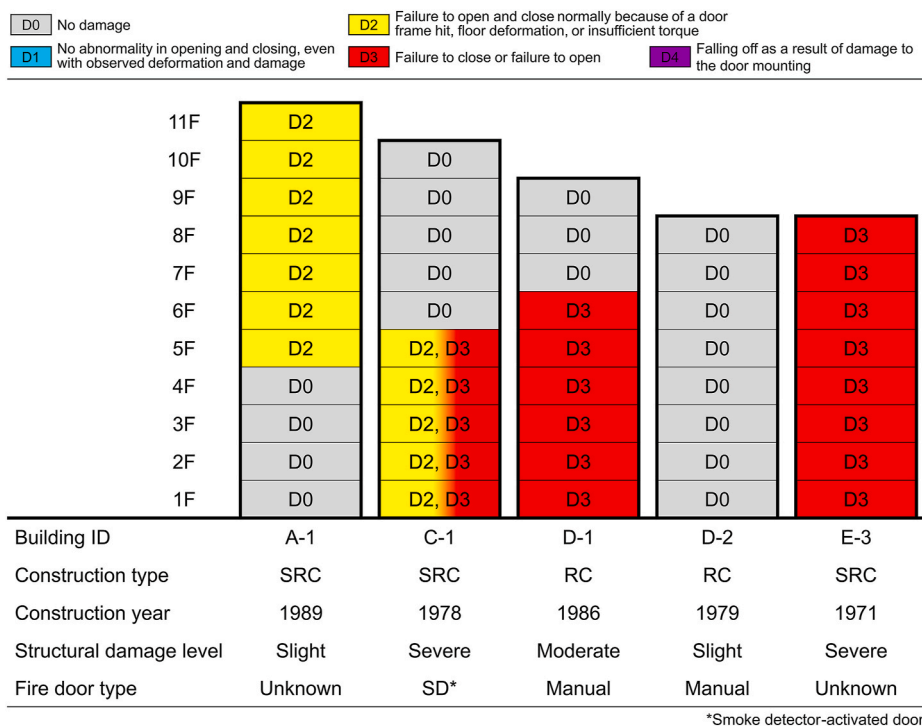


Fig. 2. Fire door damage levels observed floor by floor in the inspection by the Architectural Institute of Japan [46,47] along with relevant information.

at seismic stations during the earthquake. Note that, although the ground motion simulation is sophisticated, the synthetic waveforms are limited to 0.333–2.5 Hz (in particular, frequencies above 2.5 Hz are not included) [49]. This is because the three-dimensional finite difference method implemented in the simulation requires significant computational resources to simulate high frequencies but is an effective approach for incorporating the effect of the three-dimensional subsurface structure into the simulation. Intermediate frequencies near 1 Hz are known to have a significant effect on low-rise and mid-rise buildings [48], while higher frequencies have only secondary effects. Therefore, the synthetic waveforms used here are considered sufficient for estimating the structural responses of the analyzed buildings.

3. Methodology

Fig. 4 illustrates the methodology used in this study to develop the fire door seismic fragility function. The methodology comprises two steps. The first step performs nonlinear structural response analyses for each of the two horizontal components (i.e., the fault normal and parallel components) individually, using the Matsushima–Kawase synthetic ground motion waveforms [49] to estimate the PIDA for each floor of the five considered buildings. The second step fits a fragility function to the data, i.e., the relationship between the presence or absence of fire door damage (treated as a binary variable of 1 or 0) and the estimated PIDA, using the maximum likelihood estimation. Note that, because of the lack of information concerning the building direction, we used the fault normal and parallel components of the Matsushima–Kawase waveforms as is; therefore, they may not match the longitudinal or transverse directions of the considered buildings. However, this is expected to have only a minor effect on the obtained fragility function because a preliminary analysis using 45°-rotated waveforms did not yield a significantly different fragility function; specifically, the difference in the median, which is an unknown parameter in the fragility function (described below), was less than 0.0004 rad.

As mentioned above, no structural drawings are available for the modeling of the five considered buildings. Therefore, multi-lumped-mass shear modeling is the only possible approach to reproduce the seismic response of buildings, and plausible building models using this approach need to be implemented. The Nagato–Kawase models [50] implemented in this study are a set of building models representing the RC building stock in Kobe that was developed based on the damage statistics for the 1995 Kobe earthquake. The building models comprise 12 multi-mass models with nonlinear shear springs between two adjacent floors for each category of construction year and number of stories, with different existing ratios assigned. The nonlinear springs are assumed to have so-called degrading tri-linear hysteresis type characteristics. These 12 models all have the same yield displacement and differ only in their yield shear strengths, represented by the base shear coefficients. Namely, the uncertainty in the building strength is modeled as a discrete distribution of the base shear coefficient for each category of construction year and number of stories. This discrete distribution was derived from the log-normal distribution estimated by Shibata [51] based on RC building damage data for the 1978 Miyagi-ken Oki earthquake in Japan. Specifically, Shibata's log-normal distribution was discretized into 12 bins with different existing ratios. Only the 12 representative values were then multiplicatively calibrated by fixing Shibata's coefficient of variation (i.e., the ratio of the standard deviation to the mean) such that the damage statistics of the 1995 Kobe earthquake could be explained [50].

As an example, the base shear coefficient and existing ratio of each model are summarized in Fig. 5 for the following categories: 8–10 and 11–13 story buildings constructed before and after 1982. These base shear coefficient distributions were determined such that the damage ratios (i.e., the number of severely damaged or collapsed RC buildings divided by the total number of RC buildings) calculated from the response analyses matched those observed for the 1995 Kobe earthquake, assuming a PIDA of 1/30 rad as the criterion for severe damage or collapse. Specifically, nonlinear seismic response analyses of the 12 building models were performed for each grid point where the Matsushima–Kawase synthetic waveforms [49] described in Section 2.2 were available (specifically, at 160-m intervals for the fault parallel direction and at 80-m intervals for the fault normal direction) [50]. For each grid point, the building models predicted to suffer severe damage or collapse according to the assumed criterion were identified, and their existing

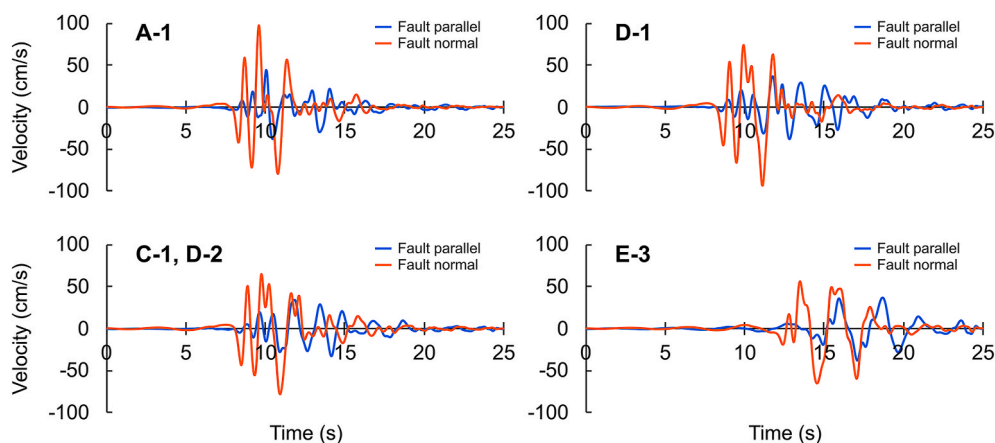


Fig. 3. Synthetic velocity waveforms used as inputs in nonlinear structural response analyses of the five buildings, with a frequency range of 0.333–2.5 Hz [49].

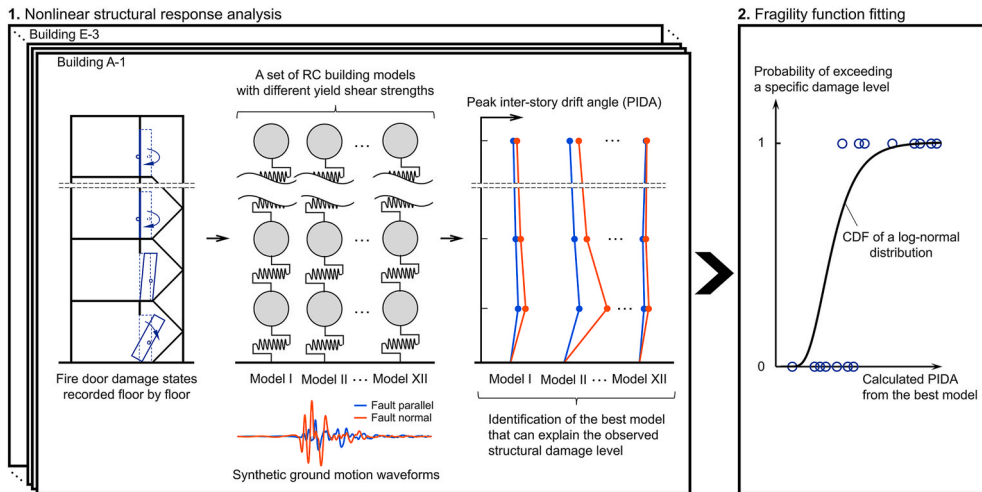


Fig. 4. Conceptual diagram of the methodology used in this study to develop the empirical fire door seismic fragility function.

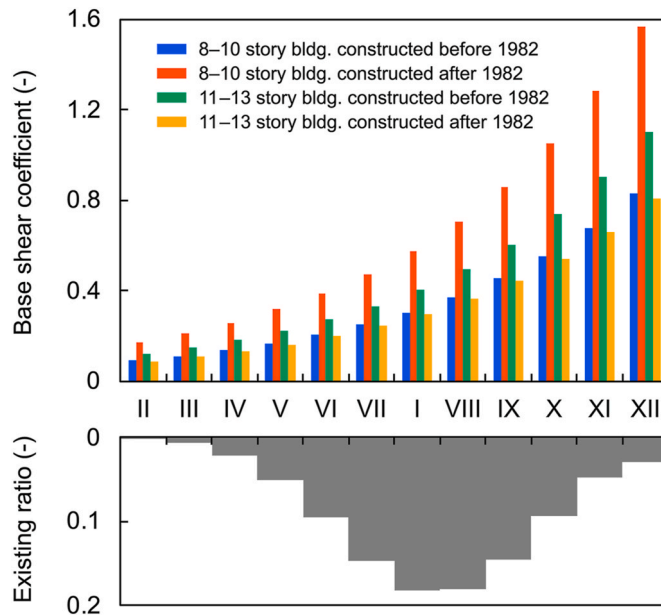


Fig. 5. Base shear coefficients and existing ratios of the Nagato-Kawase Japanese reinforced concrete building models [50].

ratios were summed [50]. The average of these sums, weighted by the actual number of buildings corresponding to each grid point, was then obtained as the calculated damage ratio for the entire region [50], which was then compared with the observed damage ratio to determine the base shear coefficient distribution. Namely, the Nagato-Kawase models characterize uncertainty in the “actual” yield shear strengths as different discrete distributions depending on the category of the construction year and number of stories. Notably, they found that the estimated average building strengths should be much higher than those considered in the design code because of the possible contribution of nonstructural walls [50]. Additional details can be found in the literature [50].

To estimate plausible PIDAs, this study identified the model that best explained the observed structural damage level from the Nagato-Kawase models for each of the five buildings. The procedure was as follows. (1) First, the PIDAs in the fault normal and parallel directions were calculated for each floor using each of the 12 models. (2) Next, models were selected for which the maximum of the calculated PIDAs for the entire building corresponded to the observed structural damage level. (3) Finally, the model with the largest existing ratio among the selected models was adopted as the best model. As for the correspondence to the observed structural damage level, the Nagato-Kawase models assume 1/100 rad and 1/30 rad as the yield story drift angle and the criterion for severe damage or collapse, respectively. Following this assumption, this study assumed that the maximum of the calculated PIDAs for the entire building must be 1/30 rad or more, 1/100–1/30 rad, and less than 1/100 rad for severely, moderately, and slightly damaged buildings,

respectively. Of course, the PIDAs estimated by even the best model have a certain amount of error, the quantification of which is left to future work. However, because the best model identification was constrained by the observed structural damage level, the estimated PIDAs are expected to be calibrated to a reasonable range.

Note that, to consider the different dynamic characteristics for buildings with different heights, Nagato and Kawase [50] classified the number of stories into four categories and assumed that a building with n stories could represent n -story buildings and $(n \pm 1)$ -story buildings. Specifically, they used models with 3, 6, 9, and 12 stories (masses) in the analysis as a representative of each category and calibrated their yielding capacities based on the observed damage ratios. In this study, for the analysis of $(n \pm 1)$ -story buildings, we also use these representative models, as is. However, for $(n - 1)$ -story buildings, we simply neglect the simulated response quantities for the n -th floor, while for $(n + 1)$ -story buildings, we assume that the simulated response quantities for the $(n + 1)$ -th floor are the same as those for the n -th floor.

Following typical fragility function fitting procedures [38,39], the observed fire door damage on each floor of the five considered buildings is linked to the calculated PIDA using the cumulative distribution function of a log-normal distribution. Let θ_{ij} be the maximum of the calculated PIDAs in the fault normal and parallel directions for the j -th floor of the i -th building. The probability of the damage state of the fire door on the j -th floor of the i -th building, DS_{ij} , exceeding the damage level, ds , is given as

$$P(DS_{ij} \geq ds) = \Phi \left[\frac{\ln(\theta_{ij}/\alpha)}{\beta} \right], \tag{1}$$

where $\Phi(\cdot)$ is the cumulative distribution function of a standard normal distribution, α is the median, and β is the logarithmic standard deviation.

In this study, fragility functions for $ds = D2$ and $ds = D3$ (i.e., the damage states exceeding the levels D2 and D3, respectively) were

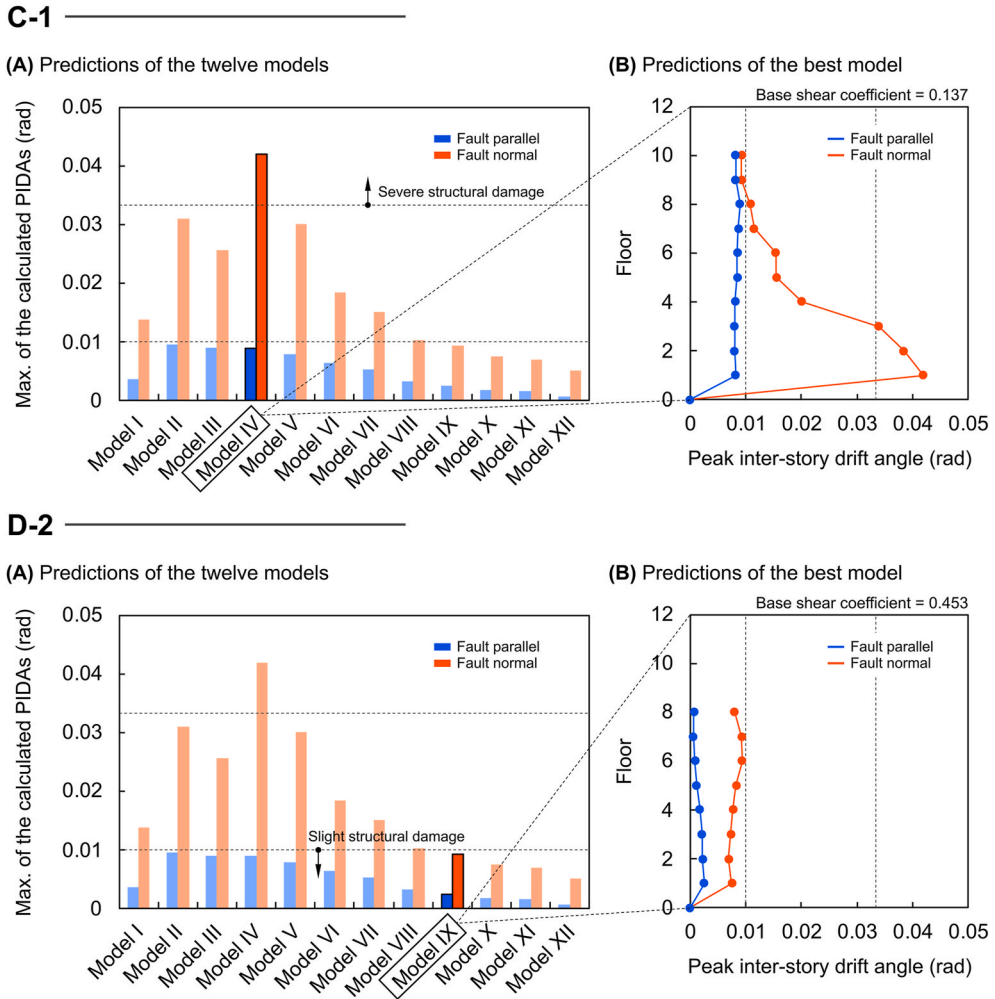


Fig. 6. Examples of identifying the best model from the Nagato-Kawase building models [50] and obtaining the plausible peak inter-story drift angles (PIDAs).

considered. When performing the fragility function fitting, some studies [39,52] have constrained the value of β between 0.2 and 0.6 for mechanical, electrical, and plumbing equipment. In the only other effort similar to this study, Miranda [45] obtained an interior door fragility function for a relatively severe damage state with a β value of 0.4. Although the fire doors in this study are different from the interior doors in Miranda’s study, the value of β in this study is fixed at 0.4 as a reference to Miranda [45] and because this value corresponds to the median of commonly used constraints. Meanwhile, the value of α is estimated such that the following likelihood function L is maximized:

$$L = \prod_i \prod_j \left\{ \Phi \left[\frac{\ln(\theta_{ij}/\alpha)}{\beta} \right] \right\}^{\Delta_{ij}} \left\{ 1 - \Phi \left[\frac{\ln(\theta_{ij}/\alpha)}{\beta} \right] \right\}^{(1-\Delta_{ij})}, \tag{2}$$

where Δ_{ij} is a binary variable that takes a value of 1 when $DS_{ij} \geq ds$ holds; otherwise, it takes a value of 0.

4. Results and discussion

Fig. 6 shows examples of identifying the best model from the Nagato–Kawase models and obtaining plausible PIDAs. For building C-1, for which the observed structural damage level was severe, the maximum of the calculated PIDAs for the entire building exceeded the criterion for severe damage (i.e., 1/30 rad) for only 1 of the 12 models with a base shear coefficient of 0.137. Therefore, this model, simulating a remarkably large drift on the lower floors, was adopted as the best model of building C-1 that can plausibly explain the observed structural damage level. For building D-2, for which the observed structural damage level was slight, the maximum of the calculated PIDAs for the entire building was less than the assumed yield story drift angle (i.e., 1/100 rad) for 4 of the 12 models. Therefore, the model with the largest existing ratio among these four models was adopted as the best model of building D-2; this model has a base shear coefficient of 0.453. As expected, the best models for these two buildings generated larger PIDAs in the fault normal direction than in the fault parallel direction for all floors. The same applies to the other three buildings. Therefore, θ_{ij} , as the explanatory variable of the fragility function, is given by the calculated PIDA in the fault normal direction for all buildings and all floors (hereinafter simply referred to as the calculated PIDA omitting the direction). Note that the installation direction of the fire doors in these buildings may not have matched the fault normal direction. However, because, as described above, a preliminary analysis using 45°-rotated waveforms did not yield a significantly different fragility function, the difference between the fire door installation direction and the fault normal direction is not expected to significantly increase the uncertainty included in the fragility function.

Fig. 7 shows the developed fire door seismic fragility function in comparison with the data. The values of α were estimated to be 0.0094 and 0.0117 for $ds = D2$ and $ds = D3$, respectively. The calculated PIDAs for the data range from 0.006 rad to 0.042 rad, mostly concentrating between 0.006 rad and 0.016 rad, where the Y-axis values are either 0 or 1, indicating uncertain damage to the fire doors. Conversely, when the calculated PIDAs exceed 0.016 rad, all data points have a Y-axis value of 1, indicating that the fire doors are definitely damaged. The developed fragility function roughly captures these data tendencies. To visually confirm the goodness of fit to the data, the data were binned and the relative frequency of data with a Y-axis value of 1 was calculated for each bin, as shown by the step functions in Fig. 7. The developed fragility function reasonably corresponds to these binned data tendencies, indicating a good fit to the data.

The data used in this study do not cover PIDAs smaller than 0.006 rad; this would require additional data to verify the applicability of the developed fragility function to smaller PIDAs. Accordingly, data from shaking table tests on a full-scale six-story building with fire-rated doors by Wang et al. [35] were plotted for comparison. The experiments show that there was no damage or slight damage inflicted on the fire-rated doors on floors with very small (0.0004–0.0006 rad) or small (0.0046 rad) observed PIDAs; meanwhile, some of the fire-rated doors failed to open because of door jamming, door frame distortion, or door latch failure on the floors with observed

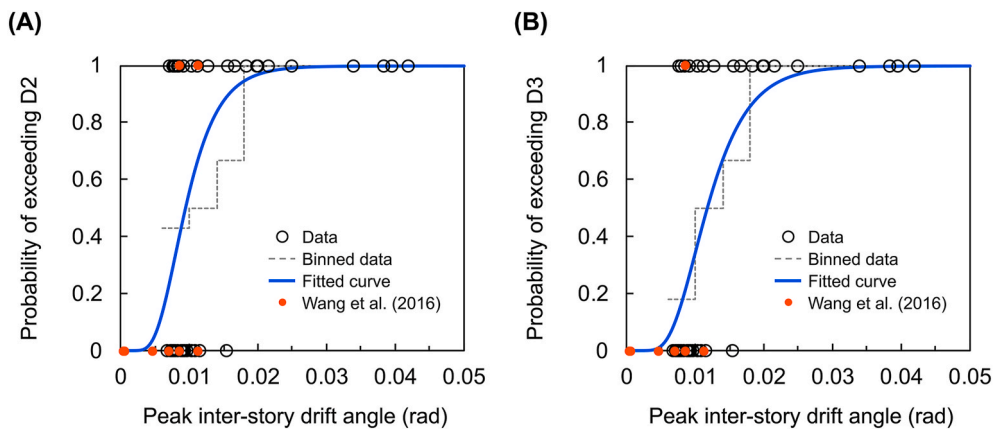


Fig. 7. Developed fire door seismic fragility function for the damage levels (A) D2 and (B) D3 and comparisons with the data used in this study and data from the Wang et al. tests [35].

PIDAs exceeding 0.008 rad. The developed fragility function rapidly rises near a PIDA of 0.005 rad. This reasonably corresponds to Wang et al.’s experimental data. Therefore, the developed fragility function is also considered to be applicable to small PIDAs. Note that the developed fragility function based on the PIDA may not match fragility functions based on the inter-story drift angle corresponding to a failure of the door to open or close, such as Miranda’s door seismic fragility functions [45], which were determined from static loading test data.

The uncertainty included in the developed fragility function is associated with the following: (1) the estimation error of the ground motion waveforms at the building locations; (2) the estimation error of the structural response of the buildings; and (3) the variation in the specification, installation, and material strength of the fire doors. First, because the analyzed buildings had no seismic records, this study used synthetic ground motion waveforms, which affected the fragility function. However, as described in Section 2.2, the synthetic waveforms were obtained via a sophisticated strong motion simulation and agreed well with those observed at seismic stations within a specific frequency range, which is limited but sufficient for analyzing the structural response of mid-rise buildings. This aspect may have minimized the effect on the fragility function. Second, because the actual yield shear strengths of the analyzed buildings are unknown, their base shear coefficients were estimated by referring to the existing building models; this affected the fragility function. However, the estimated base shear coefficients and the resulting structural responses were constrained by the observed structural damage levels of the buildings. Therefore, the PIDA values used in developing the fragility function can be considered to fall within a reasonable range. Note that this PIDA calibration is assumed to absorb the ground motion waveform estimation error; that is, the ground motion waveform estimation error and the structural response estimation error do not have a simple cumulative effect on the fragility function. The difference between the direction of the input waveform and the longitudinal or transverse direction of the building also caused an error in the structural response analysis. Finally, because the fire doors analyzed here opened into enclosed exit stairways, they were all hinged doors. However, they included different specifications and installations, such as smoke detector-activated doors (i.e., doors that are kept open in normal times) and manual doors (i.e., doors that are kept closed in normal times), which, in addition to different material strengths, affected the fragility function.

5. Case study

Here, the post-earthquake fire risk of buildings is discussed via a hypothetical case study using the developed fire door seismic fragility function. The discussion here is relative to the normal fire risk of buildings focusing on the loss of life caused by fires. The case study assumes a hypothetical building and possible fire occurrences soon after an earthquake before occupants start evacuation, yielding an analytical equation for quantifying the RFR as a function of the ground motion intensity measure and the engineering demand parameter. Of the various fire protection systems, only the fire door system is considered as a starting point for future studies because fire compartmentalization is an underlying principle in the fire safety design of buildings; however, the proposed RFR equation can easily be extended to include other fire protection systems, such as sprinkler systems. Note that the RFR assessment here is performed for buildings in Japan; specifically, the implemented models are based on statistics from Japan. However, the assessment framework is flexible, and the implemented models can be replaced depending on the given requirements.

5.1. Fire risk formulation

Consider an n -story building with two enclosed exit stairways (Fig. 8) but, for simplicity, do not consider detailed floor plans such as the location of partition walls. The considered building has an exit to the outside on the first floor. The two stairways accessible from each floor lead directly to the first floor, and the doors opening into the stairways are all smoke detector-activated fire doors. Let im be

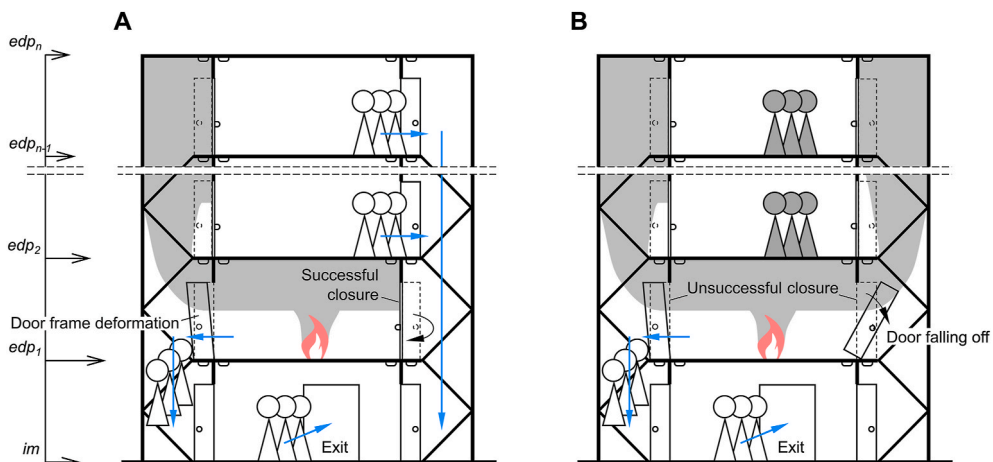


Fig. 8. Schematic of the hypothetical building assumed in the case study: (A) scenario in which one of the stairway doors on the fire floor fails to close and (B) scenario in which both of the stairway doors on the fire floor fail to close.

the ground motion intensity to which the building is subjected, and let $\mathbf{edp} = \{edp_1, edp_2, \dots, edp_n\}$ be the structural response quantity at each floor level. The building has a uniform floor area and number of occupants regardless of floor. Let A_f be the total floor area, and let ρ be the number of occupants per unit area.

Because fire protection systems are not perfectly reliable even in normal times, various fire scenarios are probable depending on the success or failure of these systems. Consequently, the expected loss of life caused by a fire is uncertain. This study therefore defines the fire risk of a building R as the sum of the products of the occurrence probability of each fire scenario and the number of casualties as a consequence of the scenario, i.e., the expected value of the number of casualties caused by fires per day:

$$R = \sum_{k=1}^m P_k L_k, \tag{3}$$

where k identifies the fire scenario, m is the number of fire scenarios, P_k is the occurrence probability of the k -th fire scenario, and L_k is the number of casualties as a consequence of the k -th fire scenario.

This study focuses on the uncertainty associated with two key elements: the fire floor (i.e., the floor where the fire originates) and the state of the stairway doors. Specifically, the fire risk is calculated by considering a set of fire scenarios as combinations of the difference in the fire floor and the success or failure of the door closing (Fig. 9). Let p_{ig} be the probability of ignition per day per unit floor area, and let p_{sdj} be the probability of a stairway door failing to close on the j -th fire floor. Assume that, only if both stairway doors on the fire floor fail to close, all occupants above that fire floor will be unable to escape to the outside via the stairways, eventually becoming fire casualties, and that otherwise, no casualties occur. Namely, the impact of the fire on the occupants on the fire floor is neglected, whereas that on the occupants above the fire floor is harshly evaluated. This is a somewhat bold assumption made to express the RFR in an analytical form as described below; however, it is not expected to cause significant problems because it emphasizes the occupants above the fire floor as potential casualties. Such occupants may be significantly more numerous than those on the fire floor and may take more time to start evacuation than those on the fire floor, especially after an earthquake. The abovementioned treatment does not require rigorous fire hazard and evacuation modeling for both post-earthquake and normal conditions, although this is a subject for future investigation. Instead, it is considered conservative and is applicable solely for simply assessing the post-earthquake fire safety level of buildings. Hence, the fire risk R is

$$R = \left(\frac{p_{ig}A_f}{n}\right) \left(\frac{\rho A_f}{n}\right) \sum_{j=1}^n p_{sdj}^2 (n-j). \tag{4}$$

Hereafter, R is used to represent the post-earthquake fire risk of a building, while R' is used to represent the normal fire risk. Assume that the post-earthquake ignition probability p_{ig} is a function of the ground motion intensity im , following existing empirical ignition models [17], while the door closing failure probability on the j -th fire floor p_{sdj} is a function of the structural response quantity at the j -th floor level edp_j . Hence, the post-earthquake fire risk R is

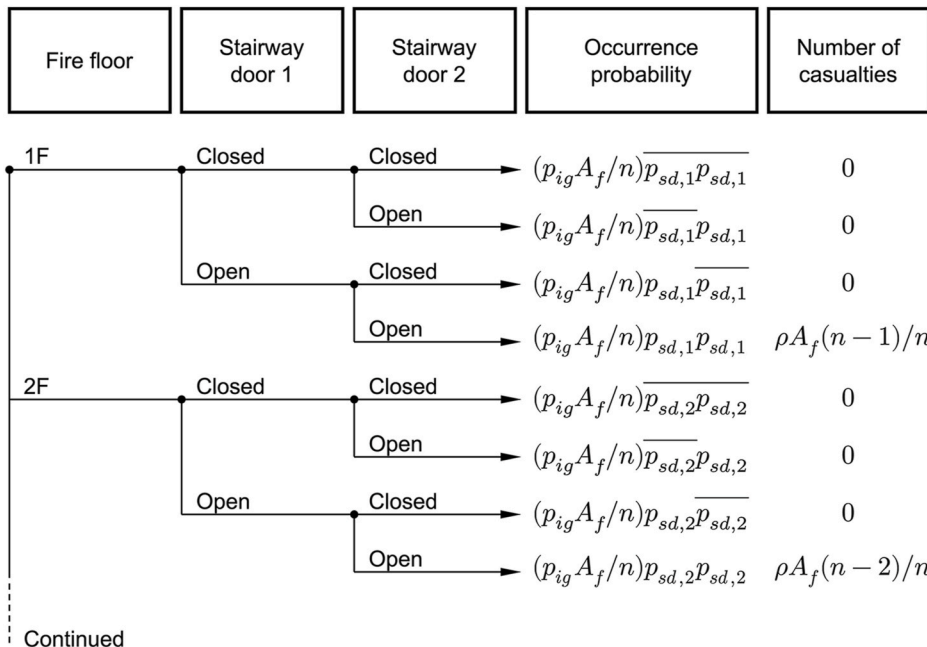


Fig. 9. Event tree diagram of the fire scenarios considered in the case study.

$$R(im, \mathbf{edp}) = \left(\frac{p_{ig}(im)A_f}{n}\right) \left(\frac{\rho A_f}{n}\right) \sum_{j=1}^n p_{sdj}^2(edp_j)(n-j). \tag{5}$$

Furthermore, let p'_{ig} be the normal ignition probability and let p'_{sd} be the normal door closing failure probability, which is assumed to be uniform regardless of floor in normal times. Hence, the normal fire risk R' is

$$R' = \left(\frac{p'_{ig}A_f}{n}\right) \left(\frac{\rho A_f}{n}\right) \sum_{j=1}^n p_{sd}^2(n-j) = \left(\frac{p'_{ig}A_f}{n}\right) \left(\frac{\rho A_f}{n}\right) \left(\frac{n(n-1)}{2} p_{sd}^2\right). \tag{6}$$

Therefore, the RFR (i.e., the ratio of the post-earthquake fire risk to the normal fire risk), denoted by R^* , is

$$R^*(im, \mathbf{edp}) = \frac{R(im, \mathbf{edp})}{R'} = \left(\frac{p_{ig}(im)}{p'_{ig}}\right) \left(\frac{2}{n(n-1)} \sum_{j=1}^n \left(\frac{p_{sdj}(edp_j)}{p'_{sd}}\right)^2 (n-j)\right). \tag{7}$$

Equation (7) shows that the RFR can be written as a function of three elements: (1) the relative ignition probability (i.e., the ratio of the post-earthquake ignition probability to the normal ignition probability); (2) the relative door closing failure probability (i.e., the ratio of the post-earthquake door closing failure probability to the normal door closing failure probability); and (3) the number of stories of the building. Calculating this equation requires models for evaluating the first and second elements. These implemented models are described in the following subsections.

5.1.1. Ignition probability

Up-to-date post-earthquake fire ignition models for Japan [17], which are regression models based on ignition records for past large earthquakes in Japan, correlate the number of shaking-related building fires that occur up to 72 h after an earthquake to the ground motion intensity, specifically the peak ground velocity (PGV), and its exposure population; that is, the 3-day post-earthquake ignition probability per person is modeled as a function of the PGV (Fig. 10). In contrast, p_{ig} and p'_{ig} , as described above, are defined as 1-day probabilities per unit floor area. Treating the modeled 3-day post-earthquake ignition probability as a 1-day probability is thought to have only a minor effect on the scope of this study because ignition incidents, which may vary in their initiation time, have been observed to be primarily concentrated in the period soon after an earthquake occurs. Therefore, this study substitutes the relative ignition probability based on the population for that based on the floor area because the normal ignition probability per person can easily be determined from national fire statistics. Hence, the relative ignition probability is modeled as

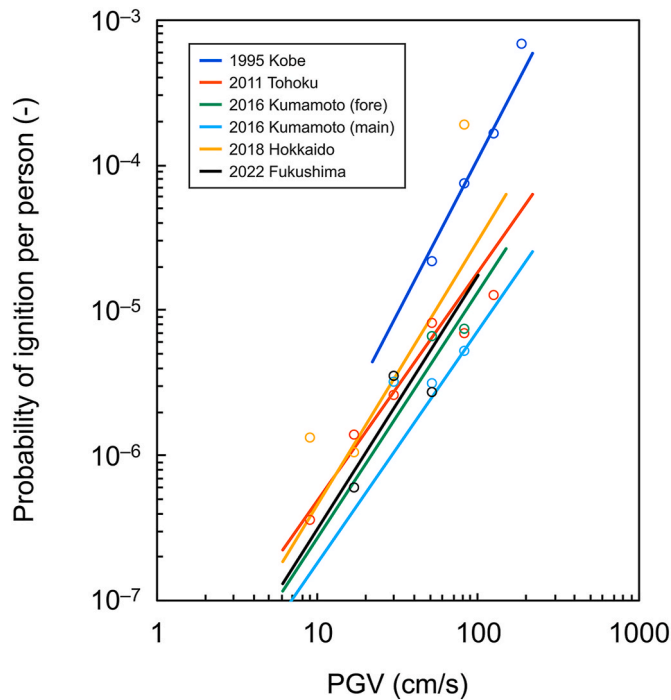


Fig. 10. Empirical relationships between the 3-day post-earthquake ignition probability per person and the peak ground velocity (PGV) derived from ignition records for recent earthquakes in Japan [17].

$$\frac{p_{ig}(im = pgv)}{p'_{ig}} \approx \frac{\exp(a + b \times \ln(pgv))}{4 \times 10^{-7}}, \tag{8}$$

where the numerator on the right-hand side represents the form of existing post-earthquake fire ignition models [17], which adopt the PGV (in cm/s) as *im* and have two parameters, *a* and *b*, calibrated for each past earthquake event, and the denominator on the right-hand side represents the normal ignition probability determined from national fire statistics, approximately 0.4 building fires per day per 1 million people on average, excluding arson or suspected arson fires. In this case study, the ignition model for the 2011 Tohoku earthquake was selected from the models of six major large earthquakes in Japan from 1995 to 2022 because this earthquake is the most recent earthquake that led to large-scale disasters and had a large number of post-earthquake fire observations.

5.1.2. Door closing failure probability

First, consider normal times. The probability of the successful functioning of a smoke detector-activated fire door is typically expressed as a product of the probability of activation upon the occurrence of a fire, denoted by p'_{ac} , and the probability of a door closing under activation, denoted by p'_{cl} . The former represents the activation reliability of a system including a detector, receiver, and electrical wiring, while the latter represents the probability of uncontrolled goods as obstacles not existing around the door, i.e., the goodness of fire safety management. Kakegawa [53] estimated p'_{ac} and p'_{cl} to be 0.93 and 0.97, respectively, based on Japanese inspection data for automatic fire alarm systems and fire doors. Using these results, the normal door closing failure probability p'_{sd} is

$$p'_{sd} = 1 - p'_{ac}p'_{cl} \approx 0.098. \tag{9}$$

Next, consider the post-earthquake probabilities. Let p_{ac} be the probability of activation upon the occurrence of a post-earthquake fire, and let p_{cl} be the probability of a door closing under post-earthquake activation. p_{ac} can decrease with respect to the probability of activation in normal times p'_{ac} as a result of possible seismic damage to the detectors, receivers, and electrical wiring. Fragility functions for such fire protection-related components are summarized in the literature [54] as a function of either the peak ground acceleration or the zero period acceleration. Although they are useful for modeling p_{ac} using a fault tree approach, their applicability to Japanese buildings is unclear. This study therefore provisionally assumes $p_{ac} \approx p'_{ac}$, and more accurate modeling is left to future work. Note that the post-earthquake activation reliability of detectors and receivers can be considered to be independent of the commercial power supply because they are typically equipped with built-in rechargeable batteries as an emergency power source. Conversely, p_{cl} incorporates the effect of possible seismic damage to the door using the developed fragility function described in Section 4, in addition to the possible existence of obstacles. Denoting the PIDA for the *j*-th floor as $pida_j$, the post-earthquake door closing failure probability p_{sdj} is

$$p_{sdj}(edp_j = pida_j) = 1 - p_{ac}p_{cl} \approx 1 - p'_{ac} \left(1 - \Phi \left(\frac{\ln(pida_j / \alpha)}{\beta} \right) \right) p'_{cl}, \tag{10}$$

where $\Phi(\cdot)$ is the cumulative distribution function of the standard normal distribution and α and β are constants. Here, $\alpha = 0.0094$ and $\beta = 0.4$, such that the damage level D2 defined in Section 2.1 can be exceeded.

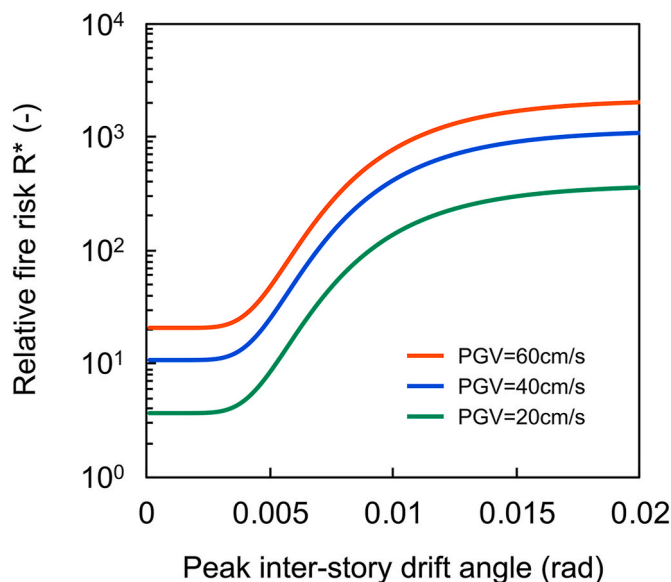


Fig. 11. Relative fire risk of buildings with varying peak inter-story drift angles (PIDAs) calculated for several peak ground velocities (PGVs).

Using Kakegawa's estimates, Eq. (10) can be summarized as

$$p_{sd,j}(edp_j = pida_j) = 0.098 + 0.902 \times \Phi\left(\frac{\ln(pida_j/\alpha)}{\beta}\right). \quad (11)$$

Hence, the relative door closing failure probability is modeled as

$$\frac{p_{sd,j}(edp_j = pida_j)}{p'_{sd}} \approx 1 + 9.204 \times \Phi\left(\frac{\ln(pida_j/\alpha)}{\beta}\right). \quad (12)$$

5.2. Results and discussion

To simplify the discussion of the effect of the PGV and PIDA values on the RFR, this case study calculated the RFR by specifying the PGV and PIDA values (Fig. 11) without performing ground motion and structural response simulations. In these calculations, we assumed several PGVs covering two ground motion levels defined by the Japanese building code, i.e., level 1 ground motion (an earthquake that occurs infrequently) and level 2 ground motion (an earthquake that occurs extremely infrequently). In addition, for simplicity, we assumed that the PIDAs are uniform regardless of the floor. This is because, for buildings designed according to the Japanese building code, the PIDAs are not expected to differ significantly between floors under level 2 ground motion (e.g., a PGV of 50 cm/s), although large inter-story drift may be concentrated in the lower floors under ground motion greatly exceeding level 2. Accordingly, the RFR here is independent of the number of stories of the building n . Not surprisingly, the results show the expected relationship that the RFR increases with increasing PGV and PIDA. The increase in the RFR in the vertical direction is due to the increase in the post-earthquake ignition probability with increasing PGV; specifically, the RFR increases by a factor of up to approximately 20 as a result of the increase in the PGV. Meanwhile, the increase in the RFR in the horizontal direction, which reveals the characteristics of the fire door seismic fragility function used, is due to the increase in the post-earthquake door closing failure probability with increasing PIDA; specifically, the RFR increases by a factor of up to approximately 100 as a result of the increase in the PIDA. Accordingly, the sensitivity of the RFR to the PIDA is much greater than that to the PGV. This is because the RFR is proportional to the square of the relative door closing failure probability (associated with the PIDA), even though both the relative ignition probability (associated with the PGV) and the relative door closing failure probability are of a similar order (i.e., up to approximately 10 or 20).

Focusing on ground motion with a PGV of 60 cm/s, which approximately corresponds to level 2 ground motion, the post-earthquake fire risk was calculated to be up to approximately 2000 times higher than the normal fire risk. Notably, even if the structural response can be reduced to less than a PIDA of 0.01 rad by its improved seismic performance, the post-earthquake fire risk of this seismically designed building will still be high, up to 800 times higher than the normal fire risk, because the fire doors may not function, even at such minor structural damage levels, and the likelihood of a fire occurring temporarily increases after an earthquake. These results suggest that post-earthquake fire risk reduction via seismic design aimed at reducing structural responses is limited and that the implementation of post-earthquake ignition prevention measures and the enhancement of occupant initial firefighting capabilities are essential. Notably, given that most fire ignitions following recent earthquakes in Japan have resulted from electrical appliances, equipment, and wiring [17], preventing electricity-related ignitions is important to further reduce the post-earthquake fire risk. As an effective measure, seismic circuit breakers, which are household devices that detect shaking and automatically cut off electrical power, are recommended for installation in Japan. Another possible solution is to develop a fire door with a different design that can accommodate large inter-story drift angles. This needs to be investigated in future work. Note that, because the normal fire risk is extremely low, the post-earthquake fire risk, despite the large relative increase, may still be low as an absolute measure when looking at a single building. However, when looking at an entire city with numerous mid-rise and high-rise buildings, the effect of the large RFR may manifest somewhere in the city as a significant loss of life caused by fires.

Although this study considered buildings equipped with only a fire door system, the qualitative findings of this study apply to those equipped with additional fire protection systems, such as sprinkler systems. Naturally, the RFR is expected to increase with the number of fire protection systems installed, given the same ground motion intensity and structural response, because the post-earthquake increase in system failure probability acts as a multiplier in the RFR equation. Therefore, the results of this study are considered to be a minimum RFR level.

6. Conclusions

An empirical fire door seismic fragility function was developed based on inspection records for five mid-rise RC buildings that suffered slight to severe structural damage from the 1995 Kobe earthquake in Japan. The developed fragility function successfully correlated the fire door damage recorded floor by floor to the PIDAs estimated via nonlinear structural response analyses based on synthetic ground motion waveforms and multi-lumped-mass shear building models for Japan. The developed function indicates that 50 % of fire doors fail to open or close at a PIDA of approximately 0.01 rad. Using the developed function, the post-earthquake fire risk of buildings was discussed via a hypothetical case study in terms of the loss of life caused by fires, assuming buildings with two exit stairways compartmentalized by smoke detector-activated fire doors. The case study results highlighted (1) that the post-earthquake fire risk can increase by up to 2000 times compared with normal periods because of the increased probability of ignition and the

reduced reliability of the fire door system and (2) that, even if the structural response can be reduced to less than a PIDA of 0.01 rad by an improved seismic performance, the post-earthquake fire risk can still be high, up to 800 times higher than the normal level. These results indicate that, in addition to seismic designs aimed at reducing the structural response, the implementation of post-earthquake ignition prevention measures and the enhancement of occupant initial firefighting capabilities are essential for post-earthquake fire risk reduction.

The results of this study contribute to the advancement of post-earthquake fire risk assessments and facilitate the consideration of fire safety in the design of seismically resilient buildings. However, the results have some limitations. The developed fragility function was obtained from an empirical case study focusing on the 1995 Kobe earthquake in Japan. Consequently, it is specific to Japanese fire doors and cannot currently be generalized to different countries. Moreover, the developed fragility function, which was derived using the estimated structural response quantities, is subject to uncertainty as a result of the inherent limitations of ground motion and structural response simulations. Therefore, further investigations are needed to validate the performance of the fragility function and reduce the associated uncertainty. In addition, although rigorous post-earthquake fire hazard and evacuation modeling is left to future work, the proposed RFR equation, which is useful for making simple assessments of the post-earthquake fire safety level of buildings relative to the normal level, was derived solely based on a fire door system, neglecting additional fire protection systems, such as sprinkler systems. To extend the application of the proposed equation, the seismic fragilities of various fire protection systems need to be comprehensively incorporated into the equation. This improved equation will allow the incorporation of system recovery curves, enabling a quantitative evaluation of the long-term variation in the RFR. Namely, it is expected to contribute to the seismic resilience quantification of buildings from a fire safety perspective.

CRedit authorship contribution statement

Tomoaki Nishino: Writing – review & editing, Writing – original draft, Visualization, Methodology, Formal analysis, Conceptualization. **Aya Hada:** Writing – review & editing, Visualization, Formal analysis. **Hiroshi Kawase:** Writing – review & editing, Methodology. **Shinichi Matsushima:** Writing – review & editing, Methodology.

Declaration of competing interest

The authors declare that they have no known competing financial interests or personal relationships that could have appeared to influence the work reported in this paper.

Acknowledgments

The authors are grateful to the members of the Research Committee on Fire Safety of the Architectural Institute of Japan, who conducted the inspection after the 1995 Kobe earthquake. This work was supported by an academia–industry collaborative research program involving Kyoto University, Tokyo Polytechnic University, the Shimizu Corporation, and the Ohsaki Research Institute, Japan. The authors thank Dr. Hiroaki Notake from the Institute of Technology, Shimizu Corporation, for his assistance in obtaining the literature on the inspection records, and Dr. Takeshi Morii from the Institute of Technology, Shimizu Corporation, for providing the opportunity to begin this study. The authors also thank Martha Evonuk, PhD, from Edanz, for editing a draft of this manuscript.

List of Abbreviations

AIJ	Architectural Institute of Japan
PIDA	Peak inter-story drift angle
PGV	Peak ground velocity
RC	Reinforced concrete
RFR	Relative fire risk
SRC	Steel framed reinforced concrete

Data availability

The data that support the findings of this study are available from the corresponding author upon reasonable request.

References

- [1] H.J. Price, A.D. Sortis, M. Schotanus, Performance of the san salvatore regional hospital in the 2009 L'aquila earthquake, *Earthq. Spectra* 28 (2012) 239–256, <https://doi.org/10.1193/1.3673595>.
- [2] E. Miranda, G. Mosqueda, R. Retamales, G. Pekcan, Performance of nonstructural components during the 27 february 2010 Chile earthquake, *Earthq. Spectra* 28 (2012) 453–471, <https://doi.org/10.1193/1.4000032>.

- [3] C.C. Jacques, J. McIntosh, S. Giovannazzi, T.D. Kirsch, T. Wilson, J. Mitrani-Reiser, Resilience of the Canterbury hospital system to the 2011 Christchurch earthquake, *Earthq. Spectra* 30 (2014) 533–554, <https://doi.org/10.1193/032013EQS074M>.
- [4] D. Perrone, P.M. Calvi, R. Nascimbene, E.C. Fischer, G. Magliulo, Seismic performance of non-structural elements during the 2016 Central Italy earthquake, *Bull. Earthq. Eng.* 17 (2019) 5655–5677, <https://doi.org/10.1007/s10518-018-0361-5>.
- [5] N. Achour, M. Miyajima, Post-earthquake hospital functionality evaluation: the case of Kumamoto Earthquake 2016, *Earthq. Spectra* 36 (2020) 1670–1694, <https://doi.org/10.1177/8755293020926180>.
- [6] S.S.H. Varzandeh, M. Mahsuli, H. Kashani, K.M. Dolatshahi, M. Hamidia, Seismic performance of buildings during the magnitude 7.3 kermanshah, Iran earthquake, *J. Build. Eng.* (2024) 109522, <https://doi.org/10.1016/j.jobbe.2024.109522>.
- [7] P.D. LeGrone, An analysis of fire sprinkler system failures during the Northridge earthquake and comparison with the seismic design standard for these systems, in: *Proceedings of the 13th World Conference on Earthquake Engineering, Vancouver, August 2004. Paper 2136*.
- [8] A. Sekizawa, M. Ebihara, H. Notake, Development of seismic-induced fire risk assessment method for a building, *Fire Saf. Sci.* 7 (2003) 309–320, <https://doi.org/10.3801/IAFSS.FSS.7-309>.
- [9] C. Scawthorn, T.D. O'Rourke, F.T. Blackburn, The 1906 San Francisco earthquake and fire—enduring lessons for fire protection and water supply, *Earthq. Spectra* 22 (2006) S135–S158, <https://doi.org/10.1193/1.2186678>.
- [10] C. Scawthorn, T. Nishino, J.C. Schencking, J. Borland, Kantō daikasai: the great Kantō fire following the 1923 earthquake, *Bull. Seismol. Soc. Am.* 113 (2023) 1902–1923, <https://doi.org/10.1785/0120230106>.
- [11] C. Scawthorn, A.D. Cowell, F. Borden, Fire-related Aspects of the Northridge Earthquake. NIST GCR, National Institute of Standards and Technology, Gaithersburg, 1996, pp. 98–743. *Building and Fire Research Laboratory*.
- [12] A. Hokugo, The performance of fire protection of buildings against the fires following the Great Hanshin-Awaji Earthquake, *Fire Saf. Sci.* 5 (1997) 947–958, <https://doi.org/10.3801/IAFSS.FSS.5-947>.
- [13] S. Lee, R. Davidson, N. Ohnishi, C. Scawthorn, Fire following earthquake—reviewing the state-of-the-art of modeling, *Earthq. Spectra* 24 (2008) 933–967, <https://doi.org/10.1193/1.2977493>.
- [14] N.E. Khorasani, T. Gernay, M. Garlock, Data-driven probabilistic post-earthquake fire ignition model for a community, *Fire Saf. J.* 94 (2017) 33–44, <https://doi.org/10.1016/j.firesaf.2017.09.005>.
- [15] T. Nishino, A. Hokugo, A stochastic model for time series prediction of the number of post-earthquake fire ignitions in buildings based on the ignition record for the 2011 Tohoku earthquake, *Earthq. Spectra* 36 (2020) 232–249, <https://doi.org/10.1177/8755293019878184>.
- [16] Q. Tong, T. Gernay, A hierarchical Bayesian model for predicting fire ignitions after an earthquake with application to California, *Nat. Hazards* 111 (2022) 1637–1660, <https://doi.org/10.1007/s11069-021-05109-6>.
- [17] T. Nishino, Post-earthquake fire ignition model uncertainty in regional probabilistic shaking–fire cascading multi-hazard risk assessment: a study of earthquakes in Japan, *Int. J. Disaster Risk Reduct.* 98 (2023) 104124, <https://doi.org/10.1016/j.ijdr.2023.104124>.
- [18] R.A. Davidson, Modeling postearthquake fire ignitions using generalized linear (mixed) models, *J. Infrastruct. Syst.* 15 (2009) 351–360, [https://doi.org/10.1061/\(ASCE\)1076-0342\(2009\)15](https://doi.org/10.1061/(ASCE)1076-0342(2009)15).
- [19] C. Scawthorn, Fire following earthquake aspects of the Southern San Andreas fault Mw 7.8 earthquake scenario, *Earthq. Spectra* 27 (2011) 419–441, <https://doi.org/10.1193/1.3574013>.
- [20] J. Cousins, G. Thomas, D. Heron, W. Smith, Probabilistic modeling of post-earthquake fire in Wellington, New Zealand, *Earthq. Spectra* 28 (2012) 553–571, <https://doi.org/10.1193/1.4000002>.
- [21] T. Nishino, T. Tanaka, A. Hokugo, An evaluation method for the urban post-earthquake fire risk considering multiple scenarios of fire spread and evacuation, *Fire Saf. J.* 54 (2012) 167–180, <https://doi.org/10.1016/j.firesaf.2012.06.002>.
- [22] T. Oki, T. Osaragi, Modeling human behavior of local residents in the aftermath of a large earthquake—wide-area evacuation, rescue and firefighting in densely built-up wooden residential areas, *J. Disaster Res.* 11 (2016) 188–197, <https://doi.org/10.20965/jdr.2016.p0188>.
- [23] T. Nishino, Physics-based urban fire spread simulation coupled with stochastic occurrence of spot fires, *Stoch. Environ. Res. Risk Assess.* 33 (2019) 451–463, <https://doi.org/10.1007/s00477-019-01649-3>.
- [24] T. Nishino, Probabilistic urban cascading multi-hazard risk assessment methodology for ground shaking and post-earthquake fires, *Nat. Hazards* 116 (2023) 3165–3200, <https://doi.org/10.1007/s11069-022-05802-0>.
- [25] Japan Association for Fire Science and Engineering, *Actual Damage to Buildings. Report on Fires Following the 1995 Hyogoken-Nanbu Earthquake, 1996*, pp. 128–135. Chapter 4.
- [26] D. Yung, G.V. Hadjisophocleous, G. Proulx, Modelling concepts for the risk-cost assessment model Firecam and its application to a Canadian government office building, *Fire Saf. Sci.* 5 (1997) 619–630, <https://doi.org/10.3801/IAFSS.FSS.5-619>.
- [27] T. Tanaka, Integration of fire risk concept into performance-based evacuation safety design of buildings, *Fire Saf. Sci.* 10 (2011) 3–21, <https://doi.org/10.3801/IAFSS.FSS.10-3>.
- [28] J. Xin, C. Huang, Fire risk analysis of residential buildings based on scenario clusters and its application in fire risk management, *Fire Saf. J.* 62 (2013) 72–78, <https://doi.org/10.1016/j.firesaf.2013.09.022>.
- [29] K. Frank, M. Spearpoint, N. Challands, Uncertainty in estimating the fire control effectiveness of sprinklers from New Zealand fire incident reports, *Fire Technol.* 50 (3) (2014) 611–632, <https://doi.org/10.1007/s10694-012-0297-2>.
- [30] K.A.M. Moinuddin, J. Innocent, K. Keshavarz, Reliability of sprinkler system in Australian shopping centres—a fault tree analysis, *Fire Saf. J.* 105 (2019) 204–215, <https://doi.org/10.1016/j.firesaf.2019.03.006>.
- [31] J. MacLeod, S. Tan, K. Moinuddin, Reliability of fire (point) detection system in office buildings in Australia—a fault tree analysis, *Fire Saf. J.* 115 (2020) 103150, <https://doi.org/10.1016/j.firesaf.2020.103150>.
- [32] J. Chang, C. Chen, T. Woo, Performance test of window glass and metal door under horizontally cyclic loading, in: *Proceedings of the 13th World Conference on Earthquake Engineering, Vancouver, August 2004*, p. 1455.
- [33] T. Lee, M. Kato, T. Matsumiya, K. Suita, M. Nakashima, Seismic performance evaluation of non-structural components: drywall partitions, *Earthq. Eng. Struct. Dynam.* 36 (2007) 367–382, <https://doi.org/10.1002/eqe.638>.
- [34] E. Forcael, V.A. Gonzalez, F. Orozco, A. Opazo, C. Belmar, J. Vera, Study of structural capacity and serviceability affecting the obstruction of residential doors, *Lat. Am. J. Solid. Struct.* 11 (3) (2013) 410–436, <https://doi.org/10.1590/S1679-78252014000300004>.
- [35] X. Wang, T. Hutchinson, G. Hegemier, S. Gunisetty, P. Kamath, B. Meacham, *Earthquake and Fire Performance of a Mid-rise Cold-Formed Steel Framed Building – Test Program and Test Results: Rapid Release Report*. University of California, Department of Structural Engineering, Structural System Research Project, San Diego, 2016. Report No. SSRP-16/07.
- [36] B.J. Meacham, Post-earthquake fire performance of buildings: summary of a large-scale experiment and conceptual framework for integrated performance-based seismic and fire design, *Fire Technol.* 52 (2016) 1133–1157, <https://doi.org/10.1007/s10694-015-0523-9>.
- [37] M. Calayir, S. Selamet, Y.C. Wang, Post-earthquake fire performance of fire door sets, *Fire Saf. J.* 130 (2022) 103589, <https://doi.org/10.1016/j.firesaf.2022.103589>.
- [38] K. Porter, R. Kennedy, R. Bachman, Creating fragility functions for performance-based earthquake engineering, *Earthq. Spectra* 23 (2007) 471–489, <https://doi.org/10.1193/1.2720892>.
- [39] G. Cremen, J. Baker, Improving FEMA P-58 non-structural component fragility functions and loss predictions, *Bull. Earthq. Eng.* 17 (2019) 1941–1960, <https://doi.org/10.1007/s10518-018-00535-7>.
- [40] R. Rezvani, S. Soroushian, A.E. Zaghi, M. Maragakis, Numerical seismic fragility analysis for suspended ceilings with various geometries, *J. Build. Eng.* 54 (2022) 104627, <https://doi.org/10.1016/j.jobbe.2022.104627>.
- [41] H. Dabiri, A. Faramarzi, A. Dall'Asta, E. Tondi, F. Micozzi, A machine learning-based analysis for predicting fragility curve parameters of buildings, *J. Build. Eng.* 62 (2022) 105367, <https://doi.org/10.1016/j.jobbe.2022.105367>.

- [42] G. Blasi, D. Perrone, M.A. Aiello, Fragility curves for reinforced concrete frames with retrofitted masonry infills, *J. Build. Eng.* 75 (2023) 106951, <https://doi.org/10.1016/j.jobe.2023.106951>.
- [43] K.Y. Dai, X.H. Yu, D.G. Lu, K. Qian, Fragility functions for corroded reinforced concrete columns, *J. Build. Eng.* 82 (2024) 108124, <https://doi.org/10.1016/j.jobe.2023.108124>.
- [44] C.D. Gaudio, G.M. Verderame, Beta functions adaptation on empirical damage for a fragility model of Italian buildings, *J. Build. Eng.* 87 (2024) 108983, <https://doi.org/10.1016/j.jobe.2024.108983>.
- [45] E. Miranda, *Seismic Fragility of Building Interior Doors*. Background Document, FEMA P-58/BD-3.9.3, Federal Emergency Management Agency, Washington, 2009.
- [46] *Research Committee on Fire Safety with enlarged membership, Hyogo-ken Nanbu Earthquake: Investigation of Damage to Fire Safety Measures in Buildings*, First Report, Architectural Institute of Japan, Tokyo, 1995 (in Japanese).
- [47] *Architectural Institute of Japan, Report on the Hanshin-Awaji Earthquake Disaster (Building Series Volume 6): Fire Damage and Civil Activities, and Damage to Information Systems*, Maruzen Publishing Co., Ltd., Tokyo, 1998, pp. 183–185 (in Japanese).
- [48] H. Kawase, The cause of the damage belt in Kobe: "The basin-edge effect," constructive interference of the direct S-wave with the basin-induced diffracted/Rayleigh waves, *Seismol. Res. Lett.* 67 (5) (1996) 25–34, <https://doi.org/10.1785/gssrl.67.5.25>.
- [49] S. Matsushima, H. Kawase, Multiple asperity source model of the Hyogo-ken Nanbu earthquake of 1995 and strong motion simulation in Kobe, *Journal of Structural and Construction Engineering (Transactions of AIJ)* 65 (2000) 33–40, https://doi.org/10.3130/aijs.65.33_3 (in Japanese).
- [50] K. Nagato, H. Kawase, Damage evaluation models of reinforced concrete buildings based on the damage statistics and simulated strong motions during the 1995 Hyogo-ken Nanbu earthquake, *Earthq. Eng. Struct. Dynam.* 33 (2004) 755–774, <https://doi.org/10.1002/eqe.376>.
- [51] A. Shibata, Prediction of the probability of earthquake damage to reinforced concrete building groups in a city, in: *Proceedings of the 7th World Conference on Earthquake Engineering*, Istanbul, Turkey, vol. 4, 1980, pp. 395–402.
- [52] K. Porter, *Fragility of Mechanical, Electrical, and Plumbing Equipment Considering Installation Conditions*. Background Document, FEMA P-58/BD-3.9.10, Federal Emergency Management Agency, Washington, 2011.
- [53] S. Kakegawa, *A Study on an Evacuation Safety Evaluation Method Based on Fire Scenarios* [Doctoral Thesis], Nagoya University, Japan, 1997 (in Japanese).
- [54] G. Johnson, R. Sheppard, M. Quilici, S. Eder, C. Scawthorn, *Seismic reliability assessment of critical facilities: a handbook, supporting documentation, and model code provisions*, Technical Report (MCEER-99-0008) (1999) 392.